Journal of Engineering Management and Systems Engineering
https://www.acadlore.com/journals/JEMSE

Load Spectrum Analysis of Axial Bearings in Hydraulic Excavators with Shovel Attachments

Vesna Jovanović[1*], Dragan Marinković[2], Nikola Petrović[1], Dubravko Stojanović[1]

[1] Department of Transport Engineering and Logistics, Faculty of Mechanical Engineering, University of Niš, 18000 Niš, Serbia
[2] Institute of Mechanics, Technical University Berlin, 10623 Berlin, Germany

[*] Correspondence: Vesna Jovanović (vesna.jovanovic@masfak.ni.ac.rs)

Received: 07-10-2024 **Revised:** 08-22-2024 **Accepted:** 09-01-2024

Citation: V. Jovanović, D. Marinković, N. Petrović, and D. Stojanović, "Load spectrum analysis of axial bearings in hydraulic excavators with shovel attachments," *J. Eng. Manag. Syst. Eng.*, vol. 3, no. 3, pp. 175–182, 2024. https://doi.org/10.56578/jemse030305.

Abstract: A detailed investigation into the axial bearing load of the revolving platform in a hydraulic excavator equipped with a shovel attachment was presented in this study. A mathematical model was formulated to assess the forces acting on the bearing under various operational conditions. The analysis focuses on a 100,000 kg excavator with a 6.5 m^3 bucket, examining the contributions of kinematic chains and drive mechanisms to axial loads. Simulations of multiple positions within the working range were carried out, calculating the load spectrum, including boundary resistance, to ensure machine stability. An optimization program was developed to refine the bearing selection process by identifying equivalent loads and moments. These calculations were benchmarked against manufacturer capacity diagrams, allowing for precise selection of appropriate bearing sizes. The findings underscore the critical role of accurate load calculations in enhancing the performance, reliability, and design optimization of hydraulic excavators. This approach provides engineers with a framework for selecting bearings that can withstand complex operational stresses, thereby improving the efficiency and longevity of hydraulic machinery.

Keywords: Revolving platform; Axial bearing; Equivalent loads; Hydraulic excavator; Load spectrum analysis

1 Introduction

Hydraulic excavators are specialized equipment primarily designed for excavation. They work through a particular kinematic chain configuration, which comprises necessary components such as the revolving segment - platform (L_2), the moving segment (L_1), and the flexible multi-member manipulators (L_m), as shown in Figure 1.

As seen in Figure 1, excavators of all sizes use changeable configurations of kinematic chains in several versions for various functions. The revolving segment (platform) and platform drive mechanism remain unchanged despite these modifications in manipulator members. The tracked and wheeled moving segments (L_{11}) that excavators are equipped with are contingent upon the specific movement and support conditions. Manipulators can be equipped with an array of tools, such as buckets, tillers, grapples, hooks, hammers, and claws. Excavation work above ground uses a shovel attachment and the "away from oneself" technique. The revolving segment (L_2), which is linked to the moving segment L_1 via a rotary joint O_2, is how hydraulic excavators perform spatial manipulation. This joint belongs to the fifth class since it is an axial bearing. This is a large bearing that enables the rotation of the excavator's superstructure. It connects the upper structure of the excavator to the undercarriage. The revolving drive mechanism consists of a hydraulic motor (1) and a reduction gear (2). It transmits the driving force needed to rotate the slewing ring. The hydraulic motor provides the power, while the reduction gear adjusts the speed and torque. The drive shaft of the reduction gear is connected to an inner toothed ring (3.1) of the axial bearing that is fixed to the moving segment (L_1) and an outer ring (3.2), which is toothless and coupled to the revolving segment (L_2). Rolling objects, such as balls or rollers, are placed between the rings in one or more races. The process of selecting an axial bearing is the first step in synthesizing the revolving platform drive mechanism. Selecting this bearing is quite difficult since the excavator operates in its working area under a wide range of various situations and in a variety of postures.

Various elements have been investigated when designing the basic excavator systems. Both analytical modeling and experimental investigation of the loading acting during the digging operation were made [1, 2]. Additionally, kinematic and dynamic excavator analysis was performed using mathematical models that were established [3, 4], and drive mechanisms and control systems were developed [5–7].

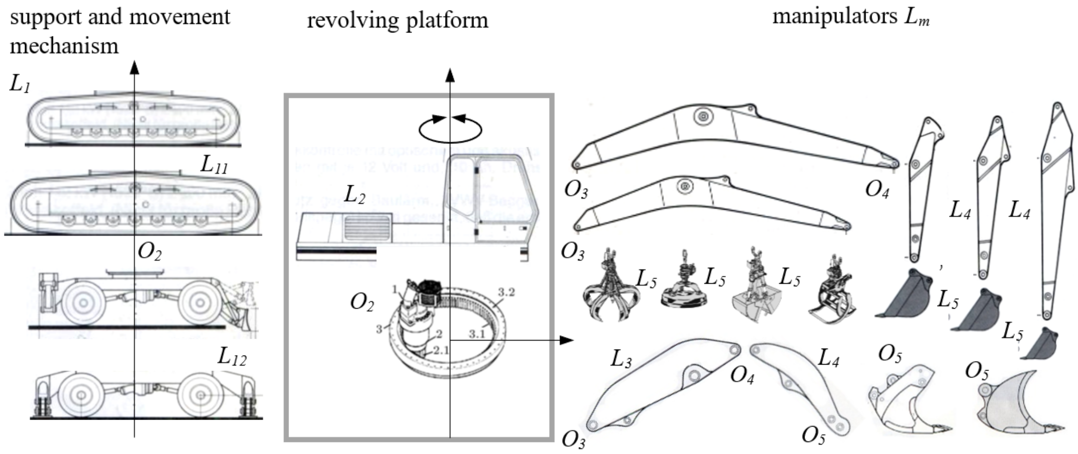

Figure 1. Variant excavator kinematic chain configurations

A recurring objective in numerous research efforts is to strike an optimal balance between simplicity and accuracy in the calculation of the load distribution on the most heavily loaded rolling elements within roller and ball bearings [8, 9]. The research also pertains to determining the axial bearings' static carrying curve. Applying the conditions to deformation compatibility and force equilibrium, Li et al. [10] established a link between the internal maximum rolling element load of each row and the total external axial load and tilting moment load of the axial bearing. The multirow geometry and a specified irregular geometry of the bearing were examined in order to determine their effects on the raceway contact load distribution. Some research has studied the effect of axial bearing machining errors on load-carrying capacities. A methodology for calculating load distribution in four-point contact axial bearings was presented by many researchers [11–13]. Load distribution was calculated, accounting for ball preload, ring flexibility and manufacturing errors, introducing a more computationally efficient approach for friction torque calculation. This demonstrates that ring deformations affect load distribution in idle but not under external loads.

Manufacturing errors in rolling elements and races affect load distribution, causing excessive local deformation and potential fatigue failure. Therefore, using the finite element method, Aithal et al. [14] revealed that ball size error and raceway waviness height are significant factors influencing load distribution.

Researchers have also examined the synthesis of the revolving platform's drive mechanism and the creation of hybrid drives for the drive mechanism, which enable energy recovery during platform slewing [15, 16].

This study provides a thorough examination of the load operating on the axial bearing in relation to the excavator's resting position on the base. In this study, a novel method was proposed to analyze the loading of the axial bearing of the excavator's revolving platform by using the load spectra that cover the entire working range of the excavator, based on the forces covered by the excavator's drive mechanisms and the limit forces under which the excavator is still stable.

2 Mathematical Modeling for the Excavator

To facilitate the load analysis of axial bearings, a comprehensive mathematical model of an excavator was developed. This model integrates both the kinematic chain and the machine drive system. The model is composed of five distinct segments that accurately represent the kinematic configuration of the excavator. These segments include segment L_1 - support and movement mechanisms (subgraph (a) of Figure 2), segment L_2 : revolving segment - platform, and the three-segment plane manipulator, which is further subdivided into segment L_3 - boom, L_4 - arm and the last segment L_5 - bucket. The spatial orientation and coordination of the excavator model were defined within the $OXYZ$ coordinate system, utilizing unit vectors to precisely delineate the spatial configuration of the model.

The axial bearing kinematic pair's vertical axis OY coincides with the support and movement segmentrevolving segment (platform) axis of the substrate-reliant excavator, which is situated in the horizontal plane OXZ with respect to the global coordinate system. The kinematic chain excavator's segments construct slewing joints with one degree of freedom, or kinematic pairs of the fifth class.

The normal irruption joint vertical axis passes through the horizontal plane at the center of the joint O_2 kinematic pair, support and movement segment- revolving segment, and the centers of the axial bearing rolling elements that connect the support and movement segment- revolving segment of the chain. The places where the kinematic chain manipulator excavator's horizontal axis irruption passes across the symmetry plane are known as the manipulator joints' centers ($O_i, i = 3, 4, 5$). The bucket cutting edge's center, O_w, was defined as the penetration point of the cutting edge through the manipulator's plane.

In their local coordinate systems $O_iX_iY_iZ_i$, models of the kinematic chain segments L_i were defined as follows:

$$L_i = \{\vec{e}_i, \vec{s}_i, \vec{t}_i, m_i\} \quad \forall \quad i = 1, 2, 3, 4, 5 \tag{1}$$

where, $\vec{e}_i = \{e_{ix}, e_{iy}, e_{iz}\}$ is the vector of the joint axis unit section L_i, which is linked to the preceding section L_{i-1} through O_i; $\vec{s}_i = \{s_{ix}, s_{iy}, s_{iz}\}$ is the position vector of two adjacent joints of the member; $\vec{t}_i = \{t_{ix}, t_{iy}, t_{iz}\}$ is the position vector of the segment's center of mass; and m_i is the segment mass.

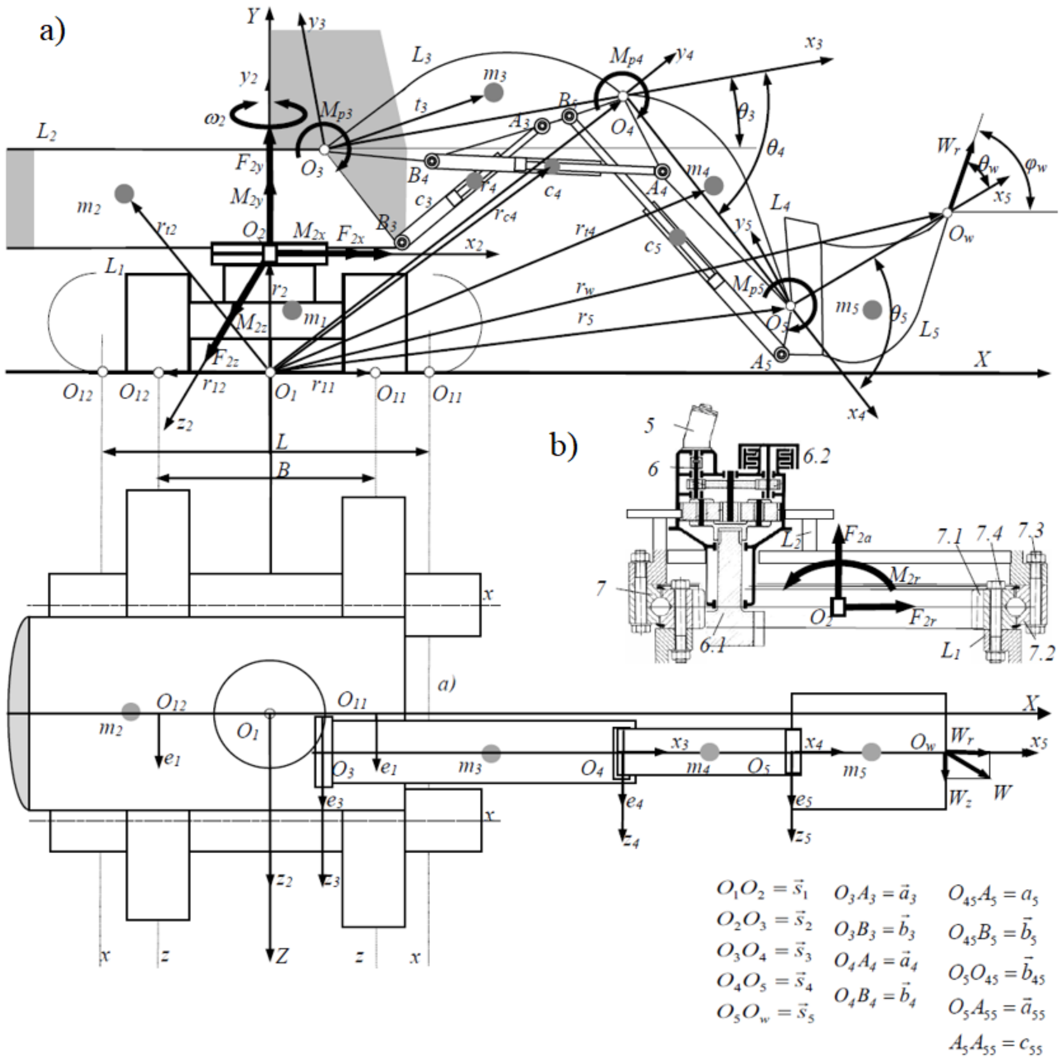

Figure 2. Axial bearing load: a) revolving platform drive mechanism; b) an excavator equipped with a shovel attachment

The driving mechanisms of the boom, arm, and bucket, which are activated by hydraulic cylinders C_3, C_4, and C_5 (subgraph (a) of Figure 2), were included in the model of the excavator's driving system. The following value sets characterize the driving mechanics of the excavator manipulator:

$$C_i = \left\{ d_{i1}, d_{i2}, c_{ip}, c_{ik}, \hat{\vec{a}}_i, \widehat{\vec{b}}_i, m_{ci}, n_{ci} \right\} \forall i = 3, 4, 5 \tag{2}$$

where, d_{i1}, d_{i2} represents the hydro-cylinder's piston and piston rod diameters; c_{ip}, c_{ik} denotes the hydrocylinder's beginning and ending lengths; $\vec{a}_i, \vec{b}_i$ represents the joint center position vectors where the hydro-cylinders are connected to the kinematic chain segments; c_i is the transmission lever length if a drive mechanism is present; m_{ci} is the hydro-cylinder mass; and n_{ci} is the number of hydro-cylinder driving mechanisms.

The kinematic chain models of the excavator are based on the following assumptions:

The substrate dependence and individual segments of the excavator kinematic chain are modeled using rigid bodies;

Digging resistance$W$ acts in the center O_w of the side of the bucket that penetrates the soil; the excavator's work is stable during manipulative tasks, meaning there is no possibility of displacement in zero-joint;

Gravitational force and digging resistance act on each member of the excavator chain during a manipulative task.

The following equation defines the vector of digging resistance:

$$\vec{W} = W_{xy} \cos \varphi_w \vec{i} + W_{xy} \sin \varphi_w \vec{j} + W_z \vec{k} \tag{3}$$

where, φ_w is the angle directions of potential digging resistance; W_z is the lateral resistance to digging; and W_{xy} is the potential resistance to digging, which acts in the manipulator's plane. The potential digging resistance is as follows [1]:

$$W_{xy} = \min \{W_s, W_3, W_4, W_5\} \tag{4}$$

where, W_s is the maximum digging resistance established for the excavator's stable operation; and W_3, W_4, and W_5 represent the maximum digging resistance it can tolerate for the boom, arm, and bucket driving mechanisms.

The following is the definition of the lateral digging resistance:

$$W_z = \frac{m \cdot g \cdot L}{4 \cdot x_w} \mu_o \tag{5}$$

where, m is the the excavator's mass; L is the length of the crawler moving mechanism; μ_o is the resistance coefficient swivel of caterpillars in relation to the base on which the excavator rests; and x_w is the horizontal coordinate the center of cutting edge of bucket.

3 Bearing Loads

The excavator's revolving platform L_2 was placed at joint O_2, and a simulated rupture of the kinematic link there leads to the ensuing force (subgraph (b) of Figure 2) to cause all weights, including the discarded components, to be redistributed toward the machine's center and the moment in joint O_2.

$$\vec{F}_2 = \vec{W} - g \sum_{i=2}^{5} m_i \vec{j} - g \sum_{i=3}^{5} m_{ci} \vec{j} - g m_z \vec{j} \tag{6}$$

$$\begin{aligned} \vec{M}_2 = &\left((\vec{r}_w - \vec{r}_2) \times \vec{W} \right) - g \sum_{i=2}^{5} m_i \left((\vec{r}_{ti} - \vec{r}_2) \times \vec{j} \right) - \\ &g m_z \left((\vec{r}_{t5} - \vec{r}_2) \times \vec{j} \right) - g \sum_{i=3}^{5} \frac{n_{ci} m_{ci}}{2} \left((\vec{r}_{ci1} - \vec{r}_2) \times \vec{j} \right) - \\ &g \sum_{i=3}^{5} \frac{n_{ci} m_{ci}}{2} \left((\vec{r}_{ci2} - \vec{r}_2) \times \vec{j} \right) \end{aligned} \tag{7}$$

where, $\vec{r}_w$ is the position vector of the center of the side of the bucket that penetrates the soil; $\vec{r}_2$ is the center joint (axial bearing) position vector O_2; $\vec{r}_{cij}$ is the position vector of the joint where the hydraulic cylinders are attached to the boom, arm and bucket; r_{ti} is the position vector of the center of mass of the chain segments; and m_z is the mass of material in the bucket (assumed that the material's and the bucket's centers of mass coincide).

The force components F_2 and moment components M_2 of the joint O_2 in X-, Y- and Z-direction are given as follows:

$$\begin{aligned} F_{2x} &= \vec{F}_2 \cdot \vec{i}, \quad M_{2x} = \vec{M}_2 \cdot \vec{i} \\ F_{2y} &= \vec{F}_2 \cdot \vec{j}, \quad M_{2y} = \vec{M}_2 \cdot \vec{j} \\ F_{2z} &= \vec{F}_2 \cdot \vec{k}, \quad M_{2z} = \vec{M}_2 \cdot \vec{k} \end{aligned} \tag{8}$$

Axial F_{2a} and radial F_{2r} force and moment M_{2r} are load components of the axial bearing revolving platforms of the excavator (subgraph (b) of Figure 2):

$$\begin{aligned} F_{2a} &= F_{2y} \\ F_{2r} &= \left(F_{2x}^2 + F_{2z}^2\right)^{0.5} \\ M_{2r} &= \left(M_{2x}^2 + M_{2z}^2\right)^{0.5} \end{aligned} \tag{9}$$

The moment M_{2z}, whose vector aligns with the bearing's axis, counterbalances the driving moment M_{p2} of the platform's revolving member. The moment M_{2x}, the vector of which lies in the horizontal plane, must also be considered. The equivalent spectrum of bearing loads was calculated, and the bearing loading capacity diagrams (curves $AL3$, $AL4$, $AL5$, and $AL6$ in Figure 2), available in the catalogs of bearing manufacturers, serve as the basis for selecting the appropriate bearing [3].

The diagram of equivalent loads is characterized by an equivalent force F_e and an equivalent moment M_e, which were determined by the following equations for F_e and M_e, respectively:

$$\begin{aligned} F_e &= (a \cdot F_{2a} + b \cdot F_{2r})\, f_s \\ M_e &= f_s \cdot M_{2r} \end{aligned} \tag{10}$$

where, a is the axial force influence factor; b is the radial force influence factor; and f_s is a factor that takes into account the working conditions of the excavator. The amount of these factors can be seen in the manufacturer's catalog for each type of bearing. They depend on the type and size of the bearing as well as on the working conditions.

4 Selection of Bearing

Only when the equivalent loads of the axial bearing are determined for all possible combinations of the kinematic chain of the excavator as well as all possible tools with which it can be equipped, can a reliably, safe and secure choice of axial bearing be made. These different combinations of manipulator members, excavator tools, and moving mechanisms are not the same as these possible kinematic chain configurations.

Given that there is digging resistance in various directions at each position of the kinematic chain depending on the excavator's operating conditions, it is necessary to ascertain the load spectrum of the axial bearing throughout the entire working space of the excavator for as many positions of the kinematic chain as feasible [17]. A computer program was developed to select the axial bearing of the revolving platform drive in hydraulic excavators and to determine the loading spectrum using the previously mentioned calculation method in order to satisfy all of the aforementioned requirements.

The number of desired positions for the machine's kinematic chains throughout the workspace, the specifications of the excavator manipulators' driving mechanisms, the maximum pressure of the excavator's hydrostatic system, and the number of resistance digging directions for the excavator enforcement tools were all entered when the program started.

According to the input values, by cyclically changing the set numbers of the kinematic chain position, the program determines: a) increments $\Delta c_i (i = 3, 4, 5)$ of the length of the hydraulic cylinders which drive boom, arm and bucket and the increment of the angle of the digging resistance force $\Delta\theta_w$; b) the length of the hydraulic cylinders $c_i (i = 3, 4, 5)$ and the angle of the digging resistance force with respect to the support base (θw); c) geometrical quantities $(\theta_i, r_i, r_{ti}, r_w)$ that define the position of the center of the joints and the center of mass of the each member of the excavator and the transmission functions of the drive mechanisms of the excavator manipulator; d) load moments and driving moments of drive mechanisms; e) limit digging resistance forces and possible digging resistance force; and f) axial bearing load components. The program allows for a detailed analysis of the equivalent loads of the axial bearing of the revolving platform drive mechanism for the desired number of kinematic chain positions in the working space of the excavator. It also allows for the desired number of changes in the possible action direction of the digging resistance force at each position through the use of spatial simulation.

Throughout the excavator's spatial simulation, the desired shift in the kinematic chain's position was achieved by cyclically altering the hydraulic cylinder lengths of the boom, arm, and bucket of the manipulator. A bearing load spectrum for the whole excavator workspace was provided by the program, corresponding to a load bearing for each kinematic chain machine position and potential digging resistance direction [18, 19]. The analysis uses parameters and diagrams of permissible load capacities of available single-row ball and roller axial bearings in possible sizes marked $AL3, \ldots, AL6$, manufactured by RotheErde [20]. To illustrate the spectrum of axial bearing loads, an excavator with a total weight of $100,000$ kg, a crawler mechanism length of $5,035$ mm, a track width of $3,600$ mm, and a bucket volume of $6.5\ \mathrm{m}^3$ was selected. The land being excavated has a density of $1,650\ \mathrm{kg/m}^3$. Longitudinal and transverse lines of overturning were observed during the load analysis. The same diagrams show the permissible load capacities of the same type but different size bearing curves $AL3$, $AL4$, $AL5$, and $AL6$ (Figure 3).

The corresponding bearing is the one under whose load-carrying curve there is a constellation of loads. As the diagrams show, the potential longitudinal line of overturning $(x - x)$ (subgraph (a) of Figure 3) is for the bearing size $AL6$, and the transverse line of overturning $(z - z)$ (subgraph (b) of Figure 3) for the bearing size $AL5$.

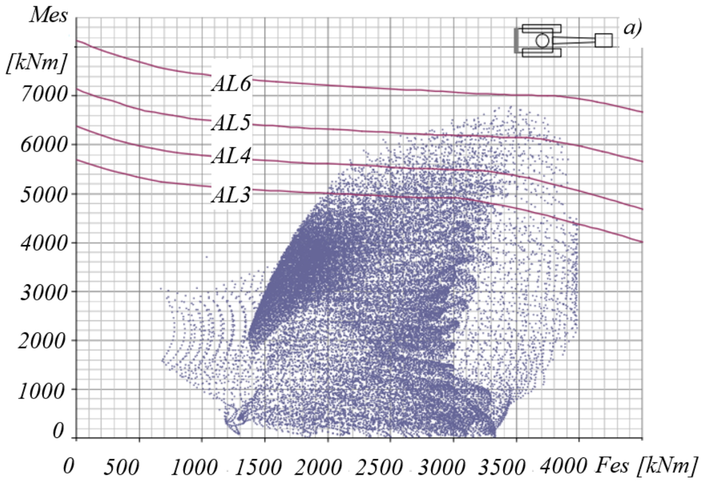

(a)

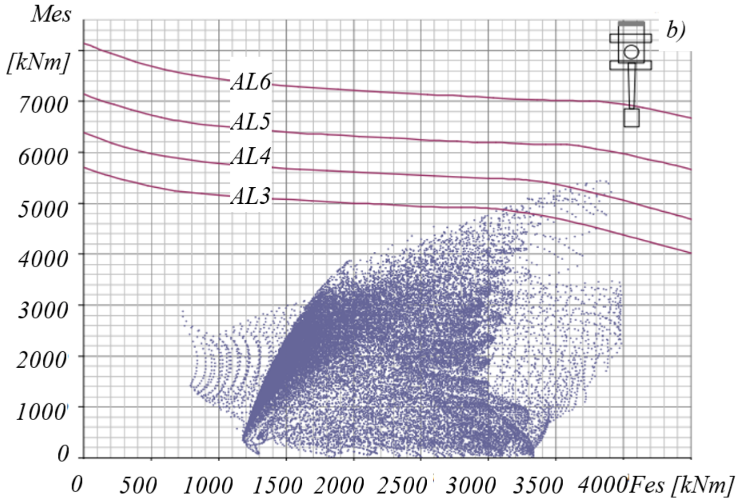

(b)

Figure 3. Load spectrums of the axial bearing revolving platform of hydraulic excavators: a) longitudinal line of overturning $x - x$, b) transverse line of overturning $z - z$

5 Conclusions

To construct the load diagram of axial bearing, a set of points was used to represent the equivalent forces and moments plots. Each point on the diagram corresponds to a specific combination of these parameters, illustrating the overall load distribution across the bearing. These calculations were performed for all manipulators that can equip the excavator for every position of the kinematic chain and all possible directions of the external load-digging forces. A comparison of the load diagrams for available bearings of identical design but varying sizes with the spectrum of operating loads provides critical insights into the bearing selection process. This comparison ensures that the chosen bearing can handle the expected loads efficiently and reliably, thus enhancing the overall performance and durability of the excavator. The selection of axial bearing is the first step in synthesizing the revolving platform mechanism. The mathematical model and software presented in this study provide a comprehensive approach to analyzing equivalent loads. This approach ensures that selected bearings meet the demanding requirements of various operational scenarios, thereby improving the performance and reliability of hydraulic excavators. Understanding and accurately calculating the loads on axial bearings is crucial for optimizing the design and selection of critical components in these complex machines. This approach to load distribution in complex mechanisms offers practical tools for engineers working with hydraulic excavators and similar machinery.

Funding

This research was financially supported by the Ministry of Science, Technological Development and Innovation of the Republic of Serbia (Grant No.: 451-03-47/2023-01/ 200109).

Data Availability

Not applicable.

Conflicts of Interest

The authors declare no conflict of interest.

References

[1] Z. Kin, "Modeling and simulation of theoretical digging force of an excavator based on arbitrary posture," *Math. Probl. Eng.*, vol. 2022, p. 8030349, 2022. https://doi.org/10.1155/2022/8030349

[2] M. Popović, I. Milićević, G. Marković, M. Marjanović, and V. Vujičić, "Load analysis for the design of cutting teeth for bucket chain excavators," in *8th International Scientific Conference Technics and Informatics in Education, Čačak, Serbia*, 2020.

[3] S. Li, S. Wang, X. Chen, G. Zhou, B. Wu, and L. Hou, "Application of physics-informed machine learning for excavator working resistance modeling," *Mech. Syst. Signal Process.*, vol. 209, p. 111117, 2024. https://doi.org/10.1016/j.ymssp.2024.111117

[4] Y. Tan, X. Chen, F. Shi, J. Wang, M. Cao, Q. Liu, and C. Wang, "Dynamic simulation analysis of working equipment of small backhoe hydraulic excavator," *J. Phys.: Conf. Ser.*, vol. 2691, p. 012007, 2024. https://doi.org/10.1088/1742-6596/2691/1/012007

[5] T. Qin, Y. Ma, Y. Li, and L. Quan, "Torque equilibrium position closed-loop control of dual electric motors swing system for large mining excavator," *Mechatronics*, vol. 95, p. 03035, 2023. https://doi.org/10.1016/j.mechatronics.2023.103035

[6] K. Hiraoka, T. Yamamoto, M. Kozui, K. Koiwai, and K. Yamashita, "Design of a database-driven assist control for a hydraulic excavator considering human operation," *J. Robot. Mechatron.*, vol. 35, pp. 703–710, 2023. https://doi.org/10.20965/jrm.2023.p0703

[7] G. Liu, Q. Wang, T. Wang, B. Li, and X. Xi, "Vision-based excavator pose estimation for automatic control," *Autom. Constr.*, vol. 157, p. 105162, 2024. https://doi.org/10.1016/j.autcon.2023.105162

[8] R. Tomović, "Load calculation of the most loaded rolling element for a rolling bearing with internal radial clearance," *Appl. Sci.*, vol. 10, no. 19, p. 6934, 2020. https://doi.org/10.3390/app10196934

[9] X. L. Ren, J. Zhai, and G. Ren, "Calculation of radial load distribution on ball and roller bearings with positive, negative and zero clearance," *Int. J. Mech. Sci.*, vol. 131-132, pp. 1–7, 2017. https://doi.org/10.1016/j.ijmecsci.2017.06.042

[10] Y. Li, R. Wang, and F. Mao, "Calculation method for the static carrying curve of double-row different-diameter ball slewing bearings," *Sci. Prog.*, vol. 106, no. 2, 2020. https://doi.org/10.1177/00368504231180026

[11] R. Potocnik, P. Goncz, and S. Glodez, "Static capacity of a large double row slewing ball bearing with predefined irregular geometry," *Mech. Mach. Theory*, vol. 64, pp. 67–79, 2013. https://doi.org/10.1016/j.mechmachtheory.2013.01.010

[12] I. Heras, J. Aguirrebeitia, and M. Abasolo, "Friction torque in four contact point slewing bearings: Effect of manufacturing errors and ring stiffness," *Mech. Mach. Theory*, vol. 112, pp. 145–154, 2017. https://doi.org/10.1016/j.mechmachtheory.2017.02.009

[13] I. Heras, J. Aguirrebeitia, M. Abasolo, I. Coria, and I. Escanciano, "Load distribution and friction torque in four-point contact slewing bearings considering manufacturing errors and ring flexibility," *Mech. Mach. Theory*, vol. 137, pp. 23–36, 2019. https://doi.org/10.1016/j.mechmachtheory.2019.03.008

[14] S. Aithal, N. Siva Prasad, M. S. Shunmugam, and P. Chellapandi, "Effect of manufacturing errors on load distribution in large diameter slewing bearings of fast breeder reactor rotatable plugs," *J. Mech. Eng. Sci.*, vol. 230, no. 9, pp. 1449–1460, 2016. https://doi.org/10.1177/0954406215579947

[15] C. Joo and M. Stangl, "Application of power regenerative boom system to excavator," in *10th International Fluid Power Conference, Dresden*, 2016, pp. 175–184.

[16] W. Li, B. Cao, Z. Zhu, and G. Chen, "A novel energy recovery system for parallel hybrid hydraulic excavator," *Sci. World J.*, vol. 2014, no. 27, p. 184909, 2014. http://doi.org/10.1155/2014/184909

[17] V. Jovanović, D. Janošević, and J. Pavlović, "Analysis of the influence of the digging position on the loading of the axial bearing of slewing platform drive mechanisms in hydraulic excavators," *Facta Univ. Ser. Mech. Eng.*, vol. 19, no. 4, pp. 705–718, 2021. https://doi.org/10.22190/fume190225020j

[18] V. Jovanović, D. Marinković, D. Janošević, and N. Petrović, "Influential factors in the loading of the axial bearing of the slewing platform drive in hydraulic excavators," *Teh. Vjesn.*, vol. 30, no. 1, pp. 158–168, 2023. https://doi.org/10.17559/tv-20220425205603

[19] V. Jovanović, D. Janošević, and J. Pavlovic, "Analysis of the influence of slewing platform drive mechanism of hydraulic excavators on the load of the axial bearing mechanism," *IMK 14 - Res. Dev.*, vol. 24, no. 4, pp. 107–112, 2018. http://doi.org/10.5937/IMK1804107J

[20] "Catalog thyssenkrupp Rothe Erde, Slewing bearings, 2007, GmbH D-44137 Dortmund," 2007. https://www.thyssenkrupp-rotheerde.com/en/products

Nomenclature

$\vec{e}_i$	Joint axis unit vector O_i
$\vec{s}_i$	Position vector of the joint center O_{i+1}
$\vec{t}_i$	Position vector of center of mass segment
m_i	Segment mass
d_{i1}, d_{i2}	Diameter of the piston and piston rod of hydro-cylinder
c_{ip}, c_{ik}	Start and final length of hydro-cylinder
$\vec{a}_i, \vec{b}_i$	Vectors of joint center position in which the hydro-cylinders linked to the segments of the kinematic chain
$\vec{c}_i$	Length of transmission levers if a drive mechanism is present
m_{ci}	Mass of hydro-cylinder
n_{ci}	Number of hydro-cylinder driving mechanism
W	Resistance to digging
W_{xy}	Potential resistance to digging
W_z	Lateral resistance to digging
φ_w	Angle directions of possible digging resistance
W_s	Maximum limit value digging resistance
W_3	Maximum limit values for digging resistance that can overcome the driving mechanisms boom
W_4	Maximum limit values for digging resistance that can overcome the driving mechanisms arm
W_5	Maximum limit values for digging resistance that can overcome the driving mechanisms bucket
$\vec{F}_2$	Resultant force in the joint O_2 revolving platform
$\vec{M}_2$	Resultant moment in the joint O_2 revolving platform
$\vec{r}_w$	Position vector of the center of the cutting edge of bucket
$\vec{r}_2$	Position vector of the center joint (axial bearing)
r_{ti}	Position vector of the center of mass the segments of the kinematic chain
$\vec{r}_{cij}$	Position vector of the joint in which are linked hydro-cylinders of driving mechanisms for kinematic chain segments
m_z	Mass of material seized by bucket
F_{2a}	Axial force in the joint O_2 revolving platform
F_{2r}	Radial force in the joint O_2 revolving platform
M_{2r}	Moment in the joint O_2 revolving platform
F_e	Equivalent force in the joint O_2 revolving platform
M_e	Equivalent moment in the joint O_2 revolving platform
a	Factor of the axial force influence
b	Factor of the radial force influence
f_s	Factor of the bearing working conditions